Design of a confocal microfluidic particle sorter using fluorescent photon burst detection

Beno H. Kunst[a)]
MicroSpectroscopy Centre, Laboratory of Biochemistry, Wageningen University, Dreijenlaan 3, 6703 HA, Wageningen, The Netherlands

Arjen Schots
Laboratory of Molecular Recognition and Antibody Technology, Wageningen University, Binnenhaven 10, 6709 PD Wageningen, The Netherlands

Antonie J. W. G. Visser[b)]
MicroSpectroscopy Centre, Laboratory of Biochemistry, Wageningen University, Dreijenlaan 3, 6703 HA, Wageningen, The Netherlands and Department of Structural Biology, Faculty of Earth and Life Sciences, Vrije Universiteit, De Boelelaan 1087, 1081 HV Amsterdam, The Netherlands

(Received 22 September 2003; accepted 14 June 2004; published 3 September 2004)

An instrumental system is described for detecting and sorting single fluorescent particles such as microspheres, bacteria, viruses, or even smaller macromolecules in a flowing liquid. The system consists of microfluidic chips (biochips), computer controlled high voltage power supplies, and a fluorescence microscope with confocal optics. The confocal observation volume and detection electro-optics allow measurements of single flowing fluorescent particles. The output of the avalanche photodiode (single photon detector) is coupled to a real-time photon-burst detection device, which output can address the control of high voltage power supplies for sorting purposes. Liquid propulsion systems like electro-osmotic flow and plain electric fields to direct the particles through the observation volume have been tested and evaluated. The detection and real-time sorting of fluorescent microspheres are demonstrated. Applications of these biochips for screening of bacteriophages-type biolibraries are briefly discussed. © *2004 American Institute of Physics.*
[DOI: 10.1063/1.1781366]

I. INTRODUCTION

A crucial requirement for screening of cellular biolibraries is the ability to detect one single cell, analyze its characteristics in real time, and sort it subsequently. A commonly used instrument for screening and sorting single fluorescent particles is the fluorescent activated cell sorter (FACS). Fluorescent cells are suspended in a stream of tiny droplets and interrogated by an optical system. The fluorescence and/or light scattering from each droplet is detected and experimental data are stored in a computer for off-line analysis. The charged droplets can be sorted in real time using electrostatic deflectors. These instruments are widely used to screen populations of relatively large cells. Smaller cells or particles like bacteria or viruses are more difficult to screen because of lower fluorescence intensity and smaller scattering power. Recently, much progress has been made using cell sorters based on microfluidic devices[1–3] enabling the fluid-phase detection and sorting of, for instance, highly fluorescent bacteria using single-molecule detection. Single molecules have been detected by means of fluorescence in relatively large capillaries,[4–6] micrometer[7–10] and even submicrometer sized channels.[11–15]

Previous work in our laboratories reported on the detection of flowing fluorescent particles like bacteria and microspheres in a microcapillary mounted on a confocal fluorescence microscopy setup.[16] These results led to the design of a microfluidic biochip aimed at detection and sorting of relatively small particles in real time using the same confocal fluorescence microscope. The biochip is made from glass, containing a network of channels and reservoirs. The particles in aqueous solution are flown through the channels employing either electrokinetic forces or pressure. To increase the detection efficiency a technique[3,17–23] is used wherein two liquid inlets focus the particles into a narrow stream (see Fig. 1). The influx of liquid into the channels was induced by either electro-osmotic flow (EOF) or electric fields in a suppressed EOF environment.

II. DESIGN, FABRICATION AND EXPERIMENTAL SETUP

A. Design of microfluidic biochips

The biochip consists of a network of channels etched into glass (Pyrex) that are connected to reservoirs (see Fig. 2). The channels are 45–50 μm wide and 20 μm deep and the reservoirs have a diameter of 2 mm on the top. Two lithographic masks defining the channel and reservoir structures have been designed using CleWin (WieWeb software, Hengelo, The Netherlands). The chrome masks were fabri-

[a)]Author to whom correspondence should be addressed; electronic mail: niek.kunst@wur.nl
[b)]Author to whom correspondence should be addressed; electronic mail: ton.visser@wur.nl

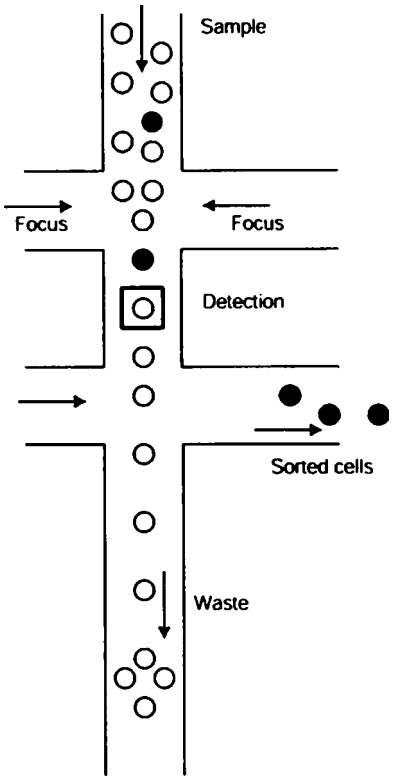

FIG. 1. Principle of fluorescent particle sorting using microfluidic channels in a glass chip.

cated using a Heidelberg DWL 200 laser beam pattern generator by Delta Mask, Enschede, The Netherlands. The glass wafers were etched in buffered HF. This anisotropic etching process requires a well-designed mask, since the channel width will eventually become the design width plus twice the etched depth. Channels on the mask were designed with a width of 5–10 μm. Etching the channels to a depth of 20 μm resulted, therefore, in channels having widths of 45–50 μm.

B. Fabrication of microfluidic devices

Microfluidic devices were fabricated out of two square 4 in. glass plates, one with a thickness of 1.1 mm and the other of 175 μm, as outlined in Fig. 3. On one side of the thick plate, a silicon layer was deposited with plasma enhanced chemical vapor deposition. Next, a photoresist layer was deposited and treated with a photolithography step to define the channel structure, which was subsequently transferred to the silicon layer by a reactive ion etching process. The patterned silicon layer was used as a masking layer in the etching of a 20-μm-deep channel in the glass plate, using an aqueous 10 wt% HF solution. Finally, the resist and silicon layers are stripped with acetone and a hot aqueous 25% KOH solution, respectively.

The backside of the plate was covered with a photoresist foil and treated with photolithography to define the reservoirs, which are subsequently machined in the glass by a powder blasting process, as previously described by Wensink *et al.*[24,25] After removal of the resist foil and thorough cleaning of the machined glass plate, it is aligned and bonded to the thin glass plate using a thermal bonding process. Finally, the wafers were diced into individual chips.

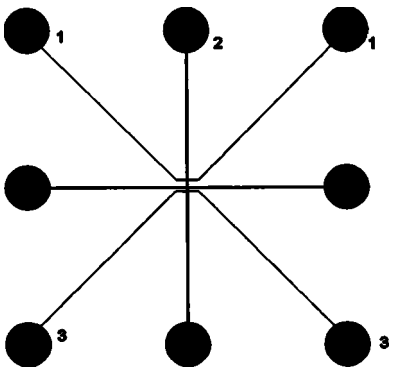

FIG. 2. Layout of a $(12.9\ \text{mm})^2$ square biochip. Eight reservoirs are connected to 50-μm-wide and 20-μm-deep channels. This particular chip design is used for experiments with emphasis on detection of single particles in combination with sorting. Reservoir 2 contains the sample, reservoirs labeled 1 are used to focus the particles into the middle of the channel and one of the reservoirs 3 is used to collect the sorted particles. The channels without numbers are not used.

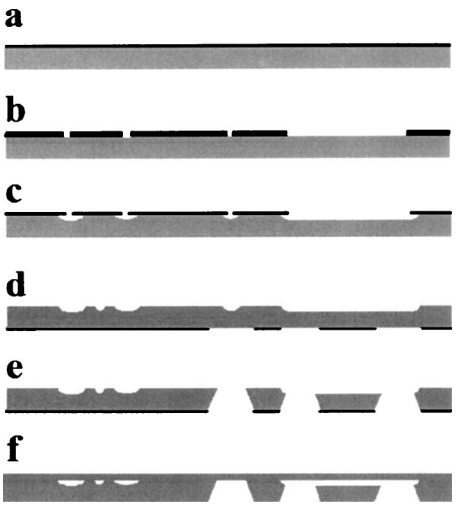

FIG. 3. Fabrication sequence. (a) Glass plate with thin silicon layer; (b) pattern transfer from photoresist to silicon layer; (c) etching of fluidic structure in glass plate; (d) photoresist pattern on backside; (e) powder blasting of structure for reservoirs in backside; (f) bonding of machined glass plate to thin glass plate.

C. Interfacing of microfluidic biochips

A special chip holder was constructed containing reservoirs, tubes, and platinum wires (see Fig. 4). The reservoirs

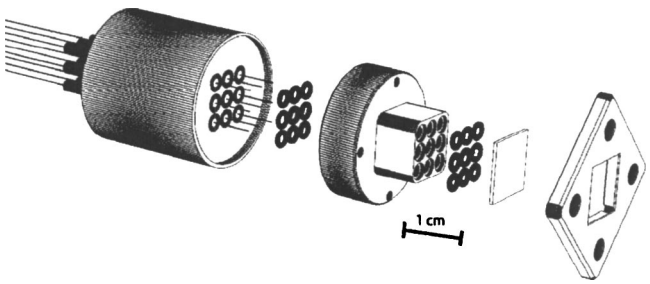

FIG. 4. Exploded view of the biochip holder. From left to right: Polymer block containing platinum wires through small tubes, set of O rings, reservoirs, set of O rings, biochip, and aluminum end plate.

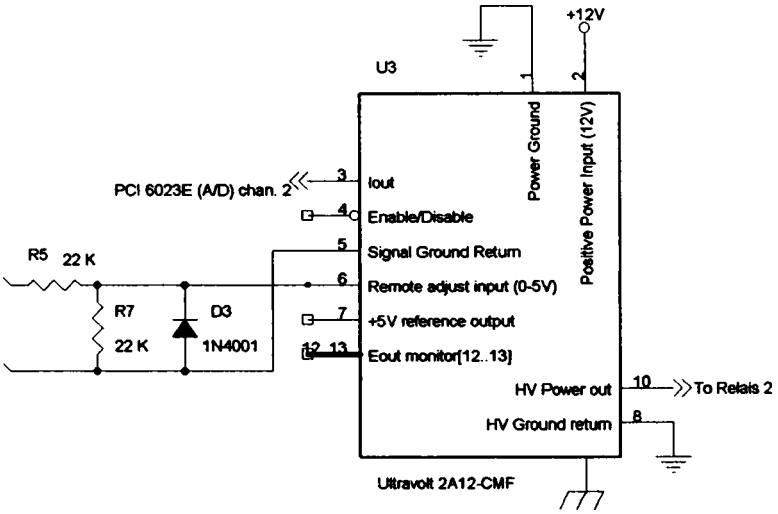

FIG. 5. Excerpt from HV power supply schematic diagram showing a protected input by a resistor and diode network.

contained up to 40 μl of liquid. The liquid flows through the biochip using either air pressure on the tubes or by electricity applied to the platinum wires.

The assembled device was placed in a piezo-controlled microscopic *xyz* translation stage (PiezoJena, Jena, Germany). With this translation stage the biochip can be moved 80 μm in all three directions with at least 100 nm precision and reproducibility. The confocal detection system consisted of an inverted fluorescence microscope (ConfoCor, Carl Zeiss, Jena, Germany, and EVOTEC Biosystems, Hamburg, Germany), especially designed to perform fluorescence correlation spectroscopy (FCS).[16,26] The 488 nm line from an argon laser was used to excite fluorescent molecules (Rhodamine Green, Rhodamine Green labeled dextrans) and fluorescent microspheres. Neutral density filters were used to decrease incident laser power when needed. Fluorescence photons were detected by an avalanche photodiode (Perkin-Elmer's optoelectronics (formerly EG&G), Quebec, Canada) and autocorrelated in real time by an AVL-5000 computer card (ALV, Langen, Germany) in a standard Windows based computer. ConfoCor software was used to control this card and to store FCS data.

D. Generation and control of electric fields

An electric field was applied to the microchannels to drive liquid or particles forward. Electric field strengths up to 500 V cm^{-1} were sufficient. Platinum electrodes from the biochip were attached to a computer controlled high voltage (HV) relay bank. These electric fields were generated using several HV modules obtained from Ultra Volt (Ronkonkoma, Long Island, NY) (see Fig. 5). The HV output from these modules can be any value between 0 and 2 kV. They take a control input of 0–5 V.

A digital-to-analog (D/A) computer card (NI-6711, National Instruments Corporation, Austin, Texas) controlled the output of the modules in combination with a homemade Labview (National Instruments Corporation) program. The analog outputs of this card can be programmed to be between 0 and 10 V and are fed into the HV modules. Since the HV modules were not protected against wrong inputs, some additional components were added. The resistor divider halved the output of the D/A card while the diode protected against wrong polarity (see Fig. 5).

Fast switching (ms range) HV relays (R1329, Celduc, Sorbiers, France) were used to switch power from different HV modules to the biochip electrodes. Switching the flow to different reservoirs was used to sort particles. The electrodes can be connected to one of the HV power supplies, to electrical ground or to nothing (floating). As a quality control parameter during experiments, the electrical current through the biochip electrodes was monitored using the current sense output from the HV modules. This output was fed into a differential input of an analog-to-digital converter computer card (NI-6023E, National Instruments Corporation). After calibration the output values were shown inside the same Labview program that drives the HV modules.

III. EXPERIMENTS

A. Real-time detection and subsequent sorting of flowing fluorescent particles

When a fluorescent particle passes through the confocal observation volume a burst of photons is emitted. A burst is defined as a minimum of x photons within a discrete time window of y seconds (typical values for x and y are 100 and 0.02, respectively). These bursts have different characteristics as compared to the background signal. The longer a particle resides in the observation volume, the more photons are emitted. This residence time is obviously correlated with the flow velocity of the particle and the size of the observation volume. The amount of photons can be estimated in a typical experiment for green-yellow microspheres[27] ($\varnothing = 1$ μm) exposing $\sim 150 \times 10^3$ fluorescent molecules (brightness of 16×10^3 photons s^{-1} molecule^{-1}) and transiting through the observation volume for 20 ms. This number amounts to $\sim 336 \times 10^3$ photons within this time period assuming an overall system detection efficiency of 0.007 using a 20× objective (Plan Neofluor, numerical aperture (NA) = 0.5, Carl Zeiss, Jena, Germany). The background signal in this time window with this objective is normally less than 20–30 photons.

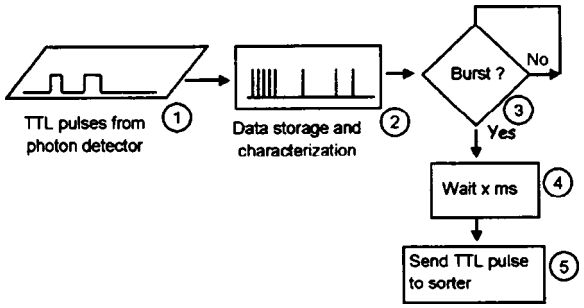

FIG. 6. Flow chart of burst detection.

The burst detection electronics consisted of two complex programmable logic devices (CPLD) (EPM7512AE, Altera, San Jose, CA) coupled to a microcontroller (C167CR, Infineon Technologies AG, Munich, Germany). These CPLDs performed several tasks like real-time detection, pipelining of positives, and driving the HV relays to sort the particles. These tasks are briefly addressed below.

The transistor-transistor logic output from the avalanche photodiode was connected to one of the CPLDs. This is represented by step 1 in Fig. 6. The microcontroller programs the CPLDs with information needed for real-time detection (time window, minimal number of photons within this time window) as well as timing parameters involved for sorting. Inside the CPLD the photons are time stamped (step 2). When a positive burst is detected (step 3), the CPLD gives a delayed (step 4) signal to the HV relays (step 5). This delay is needed since there is a time difference (because of the finite path length) between the point of detection and the channel junction for sorting. The delay and pulse duration is programmable. Since there can be more than one particle detected before sorting, a pipeline (steps 4 and 5) is included in the CPLD design. The capacity of the pipeline is circa 30-40 detection and sorting events per second.

Two of these detection systems were NANDed together to create a detection system that is capable of coincidence detection of two different fluorescent photon bursts.[28] This is useful for dual-color fluorescent labeling strategies.

B. Electro-osmotic flow in the biochip measured with FCS

Buffers of low ionic strength or salt solutions ($<$50 mM) can be pumped through the channels using either electric fields or pressure. Concerning generation of liquid flow by electricity it should be realized that the glass wall is negatively charged; positive ions from the liquid are attracted to this surface. An electric field will move these ions to the cathode thereby dragging the solution with them. This phenomenon is called electro-osmotic flow (EOF) and is influenced by the buffer composition (ionic strength and type of ions).[29] EOF can only be applied in channels smaller than $\sim$100 μm. The flow velocity of fluorescent molecules or particles through the channel can be determined with FCS as described previously.[7,16] Thus, a focused laser beam together with confocal detection optics was used to probe a tiny observation volume having a Gaussian three-dimensional (3D) intensity profile ($\sim$0.5 by 3 μm) inside the channel. Only those fluorescence photons emitted in the observation volume were detected and autocorrelated in real time yielding an autocorrelation curve. This autocorrelation curve contains information about diffusion rate and flow velocity of the fluorescent species. The theoretical framework of FCS in the analysis of uniform translation and laminar flow, superimposed on diffusion and active transport, has been given by Magde, Webb, and Elson.[30] In our case, the flow-FCS model was slightly adjusted to account for short-term phenomena like triplet-state kinetics of the molecules.[31] When there is active transport in the form of laminar flow (i.e., not turbulent), the autocorrelation function $G(\tau)$ changes to[16,32–34]

$$G(\tau) = 1 + \frac{B}{N} \cdot A \cdot e^{-[(\pi/\tau_{\text{flow}})^2 \cdot A]}, \tag{1}$$

where

$$A = \left(1 + \frac{\tau}{\tau_{\text{diff}}}\right)^{-1} \cdot \left[1 + \left(\frac{\omega_{xy}}{\omega_z}\right)^2 \cdot \left(\frac{\tau}{\tau_{\text{diff}}}\right)\right]^{-1/2}$$

and

$$B = 1 + \frac{F_{\text{trip}}}{1 - F_{\text{trip}}} \cdot e^{-\pi/\tau_{\text{trip}}}.$$

In Eq. (1) N denotes the number of fluorescent particles in the confocal observation volume (COV), τ_{flow} is the flow time, τ_{diff} is the diffusion time of the fluorescent particle (or its residence time in the COV), ω_{xy} and ω_z are the radius and length of the COV, respectively, assuming that the spatial intensity distribution of the laser beam has a Gaussian 3D profile. F_{trip} and τ_{trip} are the fraction of the molecules in the triplet state and the lifetime of the triplet state, respectively.

The flow velocity v is given by

$$v = \frac{\omega_{xy}}{\tau_{\text{flow}}}. \tag{2}$$

A 10 nM Rhodamine Green labeled 70kD-dextran was used in the flow experiments since this molecule has a relatively high molecular weight. This means that the influence of passive diffusion ($D_{\text{trans}} = 3.05 \times 10^{-11}$ m^2 s^{-1}) on the autocorrelation curve was minimized yielding a clear dependence on the flow velocity. The buffer consisted of 10 mM sodium tetraborate in water (pH=9.1). The 488 nm line of an argon laser was focused in the middle of a 50×20 μm (height $\times$ depth, respectively) channel of a biochip with a 40$\times$, NA=1.2 water immersive objective (apochromat, Carl Zeiss, Jena, Germany). The laser intensity was attenuated to approximately 40 μW with a neutral density filter. Electrical field strengths ranging from 0 to 275 V cm^{-1} have been used. The measured FCS curves showed a clear dependence on the electrical field strength. Higher electric fields displaced the autocorrelation traces to shorter times (see Fig. 7). These FCS traces were analyzed using the earlier described flow-FCS model[16] to obtain flow velocities (see Table I). The flow velocity of the liquid in the middle of the microchannel due to EOF is plotted in Fig. 8. The curve deviates from linearity at higher flow velocities due to leakage to the other open channels in the chip.

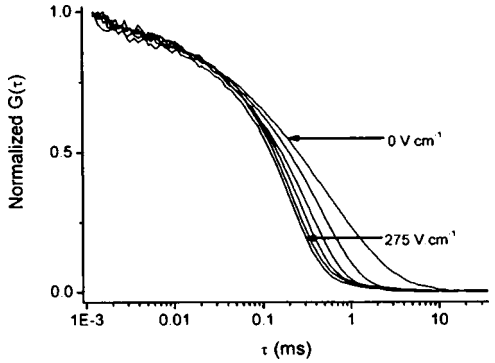

FIG. 7. Normalized autocorrelation curves (average of ten curves each collected during 10 s) of 10 nM Rhodamine Green labeled dextran (70 kD) flowing through a microfluidic channel due to electro-osmotic flow. Curves from right to left: 0–275 V cm^{-1} with incremental steps of circa 55.5 V cm^{-1}.

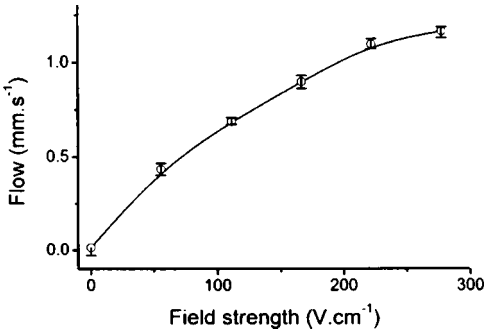

FIG. 8. Electro-osmotic flow in a biochip. The flow velocity of 10 nM Rhodamine Green labeled dextran (70 kD) in the middle of a 50×20 μm channel depends on the applied potential difference.

C. Real-time detection and sorting of flowing fluorescent microspheres

In contrast to the previous experiment where the flow velocity was determined off line from analysis of autocorrelation curves, it was desirable to measure the flow velocity in real time in order to facilitate the HV-and time-delay settings of the biochip for proper operation. For this purpose larger fluorescent particles were used. Fluorescent green-yellow microspheres or beads (diameter circa 1 μm; F8823, Molecular Probes, Leiden, The Netherlands) were suspended in buffer (10 mM sodium tetraborate, 0.03% Tween-20, pH =9.1). The nonionic detergent Tween-20 was added to suppress EOF to ensure that movement of the beads in an electric field was only due to their electric charge. The biochip (width 50 μm; depth 20 μm) was flushed with buffer and the sample reservoir filled with the suspension of beads. The electrical field strengths were at the sample -160 V cm^{-1}, focusing channels -370 V cm^{-1} and the sorting channel 530 V cm^{-1}. With these parameters, the negatively charged beads were focused into a tiny stream and deflected to the collecting reservoir. Approximately 20 particles/min were flown through the channel. The average particle velocity was determined using an intensified charge coupled device (CCD) camera (XTI, Photonics Science, East Sussex, UK) coupled to a frame grabber (Hercules 3D Prophet All-in-Wonder 9000pro, Guillemot Corp., La Gacilly Cedex, France). A mercury lamp was used for illumination through the aforementioned $20\times$ objective; spectral excitation and emission filters inside the microscope ensured that only fluorescence of the particles was imaged on the CCD. Moving particles were captured and analyzed using movie software (Premiere, Adobe Systems Inc., Seattle, WA). The average particle velocity was found to be 0.4 mm s^{-1} using the abovementioned electrical field strengths.

Once the velocity was determined, sorting the beads proved to be feasible. The $20\times$ optical objective used in the ConfoCor created an illumination volume that excited practically all focused flowing microspheres in the microchannel. Particles were detected throughout the whole depth of the channel. Excitation came from the 488 nm line of the argon laser line combined with a tenfold attenuating neutral density filter resulting in 125 μW of light energy at the sample. In Fig. 9 a typical photon burst is shown when one bead passed through the observation volume. The burst consisted of many photons emitted during transit. The burst detection threshold was set to 100 photons within a 3 ms time window. The output pulse was set to a small delay (to easily visualize correlation between detection and output pulse) and a pulse width of 20 ms.

Sorting of these 1 μm beads was demonstrated by connecting the output pulse to HV relays to switch between different collecting reservoirs. The output pulse was set according to the time needed for the particle to travel from the detection point to the channel bifurcation. It took, on average, 1.4 s for the particles to move from detection position to

TABLE I. Analysis of autocorrelation traces of a 70 kD dextran labeled with Rhodamine Green using the triplet-flow-FCS model. The following parameter values were obtained at a field strength of 0 V cm^{-1} (no flow): $F_{triplet}=0.15$, $\tau_{triplet}=2.0$ μs and a structure parameter of 5. The values of triplet and structure parameters were fixed during the analysis of autocorrelation traces in case of flow. The values between parentheses are obtained after a rigorous error analysis at the 67% confidence level; n.f.: upper limit not found.

Fieldstrength V (cm^{-1})	τ_{diff} (ms)	τ_{flow} (ms)	v mm (s^{-1})
0	0.321 (0.312–0.331)	20 (5-n.f.)	0
56	0.262 (0.249–0.274)	0.651 (0.606–0.701)	0.43 (0.40–0.46)
111	0.245 (0.235–0.254)	0.412 (0.403–0.425)	0.69 (0.67–0.71)
167	0.239 (0.225–0.252)	0.316 (0.304–0.328)	0.90 (0.85–0.93)
222	0.230 (0.217–0.244)	0.259 (0.253–0.266)	1.1 (1.1–1.1)
278	0.241 (0.231–0.253)	0.244 (0.237–0.249)	1.2 (1.1–1.2)

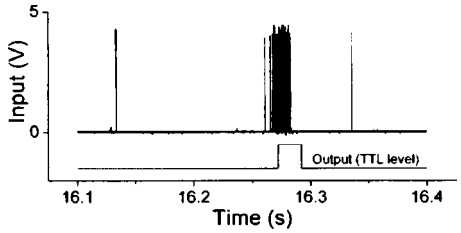

FIG. 9. Real-time detection of a fluorescent microsphere. The top graph shows the real-time output of the avalanche photodiode. This signal is attached to the detector logic. The lower graph shows the TTL output pulse (delay=0.4 ms, width=20 ms). It is connected to the reed relays logic.

sorting point (0.6 mm). The output pulse was set to a delay of 1.2 s with a width of 0.4 s. With this scheme, fluorescent particles were collected in one reservoir similarly as described recently with fluorescence imaging using a CCD camera[3] (data not shown). The sorting procedure was demonstrated to be stable for over a period of at least 2 h.

IV. DISCUSSION

Liquid flow of relatively small fluorescent particles using electro-osmotic flow (EOF) in microchannels has been clearly demonstrated. However, EOF as a tool to propel and focus small particles proved not to be successful due to interference caused by the charge of the particles and the opposite direction of the fluid flow.

Addition of detergents to the buffer reduced the EOF. The particles then moved through the liquid solely based on their electrical charge. Fast switching HV reed relays turned out to be a successful method for sorting. The used beads had a uniformly negative charge, which resulted in a uniform velocity under the influence of an electric field.

Sorting of fluorescent particles starts with their detection. The detection depends on the brightness contrast between the particles and the background. The background was very low (<5 photons per ms) compared to the signal. This is the reason why a medium power objective ($20\times$, NA $=0.5$) has been used. It created an excitation volume that allowed the detection of highly fluorescent microspheres throughout the whole channel depth. Detection and subsequent sorting of fluorescent μm-sized particles could be demonstrated given the large photon bursts despite the lower light gathering power of this objective.

Preliminary experiments using fluorescent bacteriophages having sizes of 20×60 nm showed that it is more difficult to detect and sort these much smaller particles than the highly fluorescent beads. Because of a limited degree of labeling these bacteriophages possess much lower fluorescence brightness than the microspheres. Reducing the confocal observation volume (COV) using a higher numerical aperture objective allows detection of single phages. However, this size is substantially smaller than the width and depth of the channel enhancing the probability that passing particles are not detected. When particles pass through the COV, they will not only travel fully through it, but will also partially transit the beam. This will result in uneven burst sizes with some sizes below the detection threshold. Furthermore, the two-dimensional particle focusing mechanism that is applied successfully for μm-sized beads is not working for these phages due to their small size. Possible solutions could be found in reduction of the channel dimensions,[11,12] rapid scanning of the laser beam[35,36] or by using waveguides.[37,38]

At present, the speed of detection and sorting is too low for practical use. If one wants to sort 10^5–10^6 particles from a biolibrary in a limited period of time, a different approach is required. One efficient approach would be the parallel use of thousands of microfluidic channels in a chip combined[39] with a sensitive spatial detection device such as an electron-multiplying CCD or the photon detectors directly integrated in the chip.[40] Real-time analysis of the fluorescence data can be performed by, e.g., field programmable gate arrays instead of the simpler CPLDs used in this work. Switching electric fields to sort particles with the help of reed relays in multichannel chips would not be practical, as their excessively large number would create interfacing problems. One solution would be integration of switching elements (e.g., field effect transistors) in the chip and addressing them in a multiplexed manner.

This microfluidic platform was designed to be a technology demonstrator for small particle sorting. The particles can even have a relatively low fluorescence yield that is compensated by longer interrogation times as compared to the ones used in conventional FACS machines. The microfluidic device allows screening and sorting of relatively small particles like fluorescent-labeled bacteria and viruses. Further research using these technologies to screen a small phage library is currently being undertaken in our laboratories.

ACKNOWLEDGMENTS

The authors thank Professor Dr. Albert van den Berg (Mesa+, University of Twente, Enschede, The Netherlands) for valuable advice and Micronit (Enschede. The Netherlands) for biochip fabrication. Hans de Rooij and Ing. Jacob van Otten are thanked for constructing the chip holder and the burst detector. The authors appreciated stimulating discussions with Dr. Mark Hink. This research was supported by the Dutch Technology Foundation (STW, Grant No. WBI 4797).

[1] A. Y. Fu, C. Spence, A. Scherer, F. H. Arnold, and S. R. Quake, Nat. Biotechnol. **17**, 1109 (1999).
[2] A. Y. Fu, H. Chou, C. Spence, F. H. Arnold, and S. R. Quake, Anal. Chem. **74**, 2451 (2002).
[3] P. S. Dittrich and P. Schwille, Anal. Chem. **75**, 5767 (2003).
[4] A. Castro and J. G. K. Williams, Anal. Chem. **69**, 3915 (1997).
[5] P. M. Goodwin, M. E. Johnson, J. C. Martin, W. P. Ambrose, B. L. Marrone, J. H. Jett, and R. A. Keller, Nucleic Acids Res. **21**, 803 (1993).
[6] A. Agronskaia, J. M. Schins, B. G. de Grooth, and J. Greve, Appl. Opt. **38**, 714 (1999).
[7] P. S. Dittrich and P. Schwille, Anal. Chem. **74**, 4472 (2002).
[8] C. Zander, K. H. Drexhage, K. T. Han, J. Wolfrum, and M. Sauer, Chem. Phys. Lett. **286**, 457 (1998).
[9] C. F. Chou, R. Changrani, P. Roberts, D. Sadler, J. Burdon, F. Zenhausern, S. Lin, A. Mulholland, N. Swami, and R. Terbrueggen, Microelectron. Eng. **61–62**, 921 (2002).
[10] H. P. Chou, C. Spence, A. Scherer, and S. Quake, Proc. Natl. Acad. Sci. U.S.A. **96**, 11 (1999).
[11] M. Foquet, J. Korlach, W. Zipfel, W. W. Webb, and H. G. Craighead, Anal. Chem. **74**, 1415 (2002).
[12] M. Foquet, J. Korlach, W. R. Zipfel, W. W. Webb, and H. G. Craighead, Anal. Chem. **76**, 1618 (2004).

[13] K. Dorre, J. Stephan, M. Lapczyna, M. Stuke, H. Dunkel, and M. Eigen, J. Biotechnol. **86**, 225 (2001).
[14] W. A. Lyon and S. M. Nie, Anal. Chem. **69**, 3400 (1997).
[15] M. Sauer, B. Angerer, W. Ankenbauer, Z. Foldes Papp, F. Gobel, K. T. Han, R. Rigler, A. Schulz, J. Wolfrum, and C. Zander, J. Biotechnol. **86**, 181 (2001).
[16] B. H. Kunst, A. Schots, and A. J. W. G. Visser, Anal. Chem. **74**, 5350 (2002).
[17] S. C. Jacobson, M. A. McClain, C. T. Culbertson, and J. M. Ramsey, in *Micro Total Analysis Systems 2000*, edited by A. van den Berg, W. Olthuis, and P. Bergveld (Kluwer, Dordrecht, 2000), pp. 107–110.
[18] S. C. Jacobson and J. M. Ramsey, Anal. Chem. **69**, 3212 (1997).
[19] D. P. Schrum, C. T. Culbertson, S. C. Jacobson, and J. M. Ramsey, Anal. Chem. **71**, 4173 (1999).
[20] M. A. McClain, C. T. Culbertson, S. C. Jacobson, and J. M. Ramsey, Anal. Chem. **73**, 553 (2001).
[21] J. B. Knight, A. Vishwanath, J. P. Brody, and R. H. Austin, Phys. Rev. Lett. **80**, 3863 (1998).
[22] S. A. Pabit and S. J. Hagen, Biophys. J. **83**, 2872 (2002).
[23] L. Pollack, M. W. Tate, N. C. Darnton, J. B. Knight, S. M. Gruner, W. A. Eaton, and R. H. Austin, Proc. Natl. Acad. Sci. U.S.A. **96**, 10115 (1999).
[24] H. Wensink, S. Schlautmann, M. H. Goedbloed, and M. C. Elwenspoek, J. Micromech. Microeng. **12**, 616 (2002).
[25] H. Wensink, H. V. Jansen, J. W. Berenschot, and M. C. Elwenspoek, J. Micromech. Microeng. **10**, 175 (2000).
[26] M. A. Hink, J. W. Borst, and A. J. W. G. Visser, Methods Enzymol. **361**, 93 (2003).
[27] R. P. Haugland, *Handbook of Fluorescent Probes and Research Chemicals*, 9th ed. (Molecular Probes, Eugene, OR, 2002).
[28] H. L. L. Yeng, J. J. Green, S. Balasubramanian, and D. Klenerman, Anal. Chem. **75**, 1664 (2003).
[29] B. Chankvetadze, *Capillary Electrophoresis in Chiral Analysis* (Wiley, Chichester, U.K., 1997).
[30] D. Magde, W. W. Webb, and E. L. Elson, Biopolymers **17**, 377 (1977).
[31] J. Widengren, Ü. Mets, and R. Rigler, J. Phys. Chem. **99**, 13368 (1995).
[32] M. Brinkmeier and R. Rigler, Exp. Tech. Phys. (Lemgo, Ger.) **41**, 205 (1995).
[33] M. Brinkmeier, K. Dorre, J. Stephan, and M. Eigen, Anal. Chem. **71**, 609 (1999).
[34] M. Gösch, H. Blom, J. Holm, T. Heino, and R. Rigler, Anal. Chem. **72**, 3260 (2000).
[35] K. M. Berland, P. T. C. So, Y. Chen, W. W. Mantulin, and E. Gratton, Biophys. J. **71**, 410 (1996).
[36] V. Levi, Q. Ruan, K. Kis Petikova, and E. Gratton, Biochem. Soc. Trans. **31**, 997 (2003).
[37] L. M. Fu, R. J. Yang, C. H. Lin, Y. J. Pan, and G. B. Lee, Anal. Chim. Acta **507**, 163 (2004).
[38] Y. C. Tung, M. Zhang, C. T. Lin, K. Kurabayashi, and S. J. Skerlos, Sens. Actuators B **98**, 356 (2004).
[39] D. Erickson and D. Q. Li, Anal. Chim. Acta **507**, 11 (2004).
[40] M. L. Adams, M. Enzelberger, S. Quake, and A. Scherer, Sens. Actuators, A **104**, 25 (2003).